

# Mechanism of unidirectional emission of ultrahigh Q Whispering Gallery mode in microcavities

C.-L. Zou, F.-W. Sun,\* C.-H. Dong, X.-W. Wu, J.-M. Cui, Y. Yang, G.-C. Guo, and Z.-F. Han†  
*Key Lab of Quantum Information, University of Science and Technology of China, Hefei 230026*

(Dated: October 6, 2021)

The mechanism of unidirectional emission of high Q Whispering Gallery mode in deformed circular microcavities is studied and firstly presented in this paper. In phase space, light in the chaotic sea leaks out the cavity through the refraction regions, whose positions are controlled by stable islands. Moreover, the positions of fixed points according to the critical line in unstable manifolds mainly determines the light leak out from which refraction region and the direction of the emission. By controlling the cavity shape, we can tune the leaky regions, as well as the positions of fixed points, to achieve unidirectional emission high Q cavities with narrow angular divergence both in high and low refractive index materials. Especially for high index material, almost all Gibbous-shaped cavities have unidirectional emission.

PACS numbers: 42.55.Sa, 05.45.Mt, 42.25.-p, 42.60.Da

In recent years, being the high potential elements for integrated devices, dielectric microcavities have attracted more and more attentions. Especial attentions are focused on the Whispering Gallery (WG) micro-resonators, such as micro-sphere, micro-disk, micro-toroid, etc, where energy can be well confined in these rotational symmetrical structures by total internal reflections. The unique high quality (Q) factor and low mode volume features of WG Modes lead to wild applications, ranging from nonlinear optics, low threshold lasers, sensitive sensors, to cavity quantum electrodynamics [1]. However, the isotropic emission property of WGMs makes very low efficient coupling from free space. Also, the near field coupling component is a big obstacle for practical applications. To solve the coupling problem, researchers found that the microcavity with slightly deformed circular boundary, also called asymmetric resonant cavity (ARC), can lead directional emission. The ARCs, such as the extensively studied quadruple [2, 3, 4, 5, 6] and stadium microcavities [7, 8, 9], can be efficiently pumping through free space focused beam, which makes them have been well used in the realization of strong coupling [10] and laser [11]. Besides the easy free space coupling in the optical experiments, the deformed microcavities can also serve as open billiards for experimental research on quantum chaos [12, 13].

In order to get more efficient free space excitation and collection in practical application, people are pursuing single directional emission with narrow angular divergence, such as the spiral shaped [13, 15, 16] and the rounded isosceles triangle shaped [17] microcavities. However, their low Q factors highly limit the applications in low threshold laser and cavity quantum electronic dynamics. Although there are several theoretical approaches [18, 19], the trade-off between the high Q and unidirectional emission still blocks its further development. It is till recently that fabrication-friendly limaçon-shaped microcavity with both unidirectional emission and high Q was theoretically proposed [20] and experimentally realized by several groups [21, 22, 23]. However,

the mechanism to design such cavity is not clear yet. Moreover, this limaçon-shaped microcavity is based on the high refractive index material. There is no report for high Q and unidirectional emission cavity with low index material.

In this paper, we will show the mechanism to get unidirectional emission high Q mode both in the high and low refractive index ARC. At the beginning, we summarize the necessary conditions to achieve the high Q unidirectional emission ARC. First, the cavity boundary should be continuous, smooth, and slightly deformed from a circle to support the WG-like modes. In such deformed microcavity, the wave is mainly localized high above the critical line and well confined in the cavity to support high Q. The light may leak out when the ray is lower than critical line in phase space. In this case, the rays follow the unstable manifolds, cross the critical line, and perform the directional emission tangential to the cavity boundary.

Second, the boundary shape should have less symmetry. For planar deformed cavity with two or more axial symmetries, there are at least two pairs of symmetric tangential emission spots on the boundary because they support both clockwise and counterclockwise traveling modes [2, 3, 4, 5, 6, 7, 8, 9]. The only way to achieve unidirectional emission is to design the cavity with at most one symmetric axis and make the emission direction along the axis direction.

In the cavity with continuous, smooth, and slightly deformed circular boundary, there are stable and unstable orbits, corresponding to the stable islands and fixed points of unstable manifolds in phase space. The mechanism for the unidirectional emission in the single-axis cavity is: The light only along the manifolds may leak out the cavity. Isolated by the stable islands, the manifolds have several leaky regions when they cross the critical refractive line. By controlling the cavity shape, we can tune the leaky regions, as well as the position of fixed points according to the critical line. The light through the lower fixed point has higher probability to leak out than through the higher point. The parallel leaky lights along the axis direction shows unidirectional emission from the high Q ARC. Based on this mechanism, we succeed in designing the unidirectional high Q ARC both in high and low refractive index materials. We find that almost all Gibbous-shape ARCs have unidirectional emission for high refractive index

\*Electronic address: fwsun@ustc.edu.cn

†Electronic address: zfhan@ustc.edu.cn

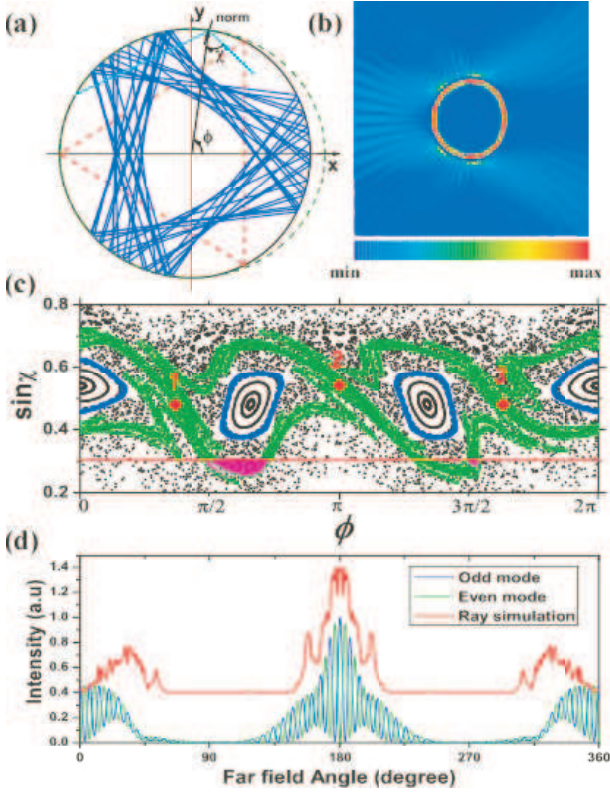


FIG. 1: (color online) (a) The real space illustration of the rays reflection inside HQHC deformed microcavity with  $\epsilon = 0.11$ . The dashed line outside is the circle boundary. The blue lines and red dash lines are the stable and unstable period-3 orbits. (b) The calculated field spatial distribution of TM polarized fundamental WG-like mode in HQHC, with the wavenumber in vacuum  $kr \approx 26.15$  and quality factor  $Q = 3.3 \times 10^5$ . (c) The phase space structure of HQHC. The blue circles and red diamonds are the stable islands and fixed points, corresponding to the stable and unstable period-3 orbits in (a). The red line is the critical refraction line with  $\sin \chi = 1/n$ , and the green points are the unstable manifolds from the unstable period-3 orbits. Magenta points is the collection records of leaky rays location from the original rays upon  $\sin \chi > 0.7$ . It shows that most rays leak out from this refraction region. (d) the far field patterns for TM polarized ray (the red line, lifted by 0.4) and wave simulation (blue line and green line for even and odd parity mode respectively).

material. By precisely controlling the boundary shape, we can achieve far field emission with very narrow divergence angle.

At first, we consider a boundary shape of Half-Quadruple-Half-Circle (HQHC) to illustrate the unidirectional emission in high refractive index cavity, which have been demonstrated in silica microsphere [24]. The slightly deformed circular boundary shape, as shown in Fig. 1(a), can be read as

$$R(\phi) = \begin{cases} R_0, & \cos \phi < 0, \\ R_0 (1 - \epsilon \cos^2 \phi), & \cos \phi \geq 0, \end{cases} \quad (1)$$

where  $\phi$  is the polar angle according to the symmetric X-axis and  $\epsilon$  is the deformation factor. In the limit of  $R \gg \lambda$ , the light in cavity can be semiclassically treated as ray. Although wave nature of light is important in microcavity, the ray dynamics

is still an efficient tool to understand and analyze the emission properties of ARCs [22, 23, 25, 26, 27, 28, 29, 30].

The sequence of ray reflection inside the cavity in real space can be represented in the phase space as Poincaré Surface of Section (SOS). Each ray reflection on the boundary is recorded in Birkhoff coordinates [31] as  $(\phi, \sin \chi)$ , where  $\phi$  and  $\chi$  denote the polar angle of reflection position on boundary and the incidence angle, respectively. By setting rays initially random on boundary (here we only consider the counterclockwise propagation rays, the clockwise SOS can be obtained by symmetric transformation), we can get the SOS by treating the cavity as billiard [12], which is shown in Fig. 1(c).

In SOS, the phase space structure can be divided into two parts, the chaotic sea and the stable islands. The two regions are isolated to each other. The ray in chaotic sea [black points in Fig. 1(c)] has chaotic motions in real space, while the ray in islands (in blue) is conserved and will never move into chaotic sea. In the real space, the stable islands are corresponding to the stable (blue solid lines) period-3 orbits [31], as shown in Fig. 1(a). The light in the chaotic sea will run along the unstable manifolds [26] [green curve in Fig. 1(c)] and leak out when it crosses critical line, which is denoted by the red line in Fig. 1(c). The critical line shows the critical incidence angle for total internal reflection  $\sin \chi = 1/n$ . We set the refractive index  $n = 3.3$  in our case.

In this slightly deformed circular cavity, the light is mainly localized upon the critical line in phase space. In the real space, the light runs in the unstable periodic orbits or high Q WG-like mode, as shown in Fig. 1(b) [20, 21, 25]. Initially, we set rays uniformly distributed in the region  $\sin \chi > 0.7$ , which can be considered as energy of high Q modes dynamics localized above the critical line. Rays will be reflected on the boundary in sequence until they hit the refraction regions. In the SOS, the refraction regions are the parts of chaotic sea below the critical line ( $\sin \chi < 1/n$ ). As the manifolds enclose the stable islands, the locations of the stable islands determine the positions of these refraction regions. In our case, the center two stable islands are lower than the third island. So, there are two refraction regions near  $\phi \approx \pi/2$  and  $3\pi/2$  at boundary, corresponding to two directional emissions with far field angles of 180 and 360 degrees.

In order to get the unidirectional emission, we need to analyze the relative positions of the three fixed points in the manifolds, as shown with red diamonds in Fig.1(c). It is corresponding to the unstable (red dashed lines) period-3 orbit [31] in Fig. 1(a). They are sandwiched by the stable islands. All lights following the manifolds will transit through/near these three points. However, the fixed point (marked as 1) before refraction region near  $\phi \approx \pi/2$  is lower than the point (marked as 2) before the other refraction region near  $\phi \approx 3\pi/2$ . Also, it is closer to the refraction region. So the manifolds here are shorter and steeper to cross the critical line. As a result, the light through/near fixed point 1 has the higher probability to enter the fraction region and leak out than the other one. It will give rise to the most energy leaky here and the directional emission with far field angle of 180 degrees. From the symmetry, the clockwise propagation rays leak out around  $\phi \approx 3\pi/2$  and show the same directional far field emission.

Therefore, the leaky beams from the counterclockwise and clockwise propagations are parallel and finally show unidirectional emission from this HQHC cavity.

With the numerical solution of Maxwell equations through boundary elements method [32, 33], we can observe the high Q WG-like mode in this HQHC microcavity. Fig. 1(b) shows the electric field intensity distribution of WG-like transverse magnetic (TM) polarized mode with radiation quantum number  $q = 1$  (the transverse electric polarized modes have the similar properties). The near field pattern shown tangent light emission from  $\phi \approx \pi/2$  and  $3\pi/2$ , corresponding to the two refraction regions. Obviously directional emission beams for (counter)clockwise propagation are along the X-axis.

The far field distribution of the Odd and Even polarity WG-mode is shown in Fig. 2(d), as well as the ray-wave correspondence with ray dynamics. In the ray simulation, with the weighted refractive coefficient from Fresnel law, we can get the far field amplitude by summing up the all refractions, as shown in Fig. 2(d) with the red curve. In order to get clear illustration, the curve is lifted by 0.4. The far field pattern shows the unidirectional emission at 180 degree with divergence about 30 degrees.

As discussed above, the refraction regions and fixed points in unstable manifolds play the most important roles to determine the cavity directional emission. So, we can tune the cavity shape to adjust the locations of stable islands and the positions of fixed points to control the refraction regions and the emission direction, simultaneously. To achieve the unidirectional emission of high Q modes, we can design the X-axis symmetric cavity and lead the unidirectional emission along the axis. In general, the boundary of X-axis symmetric shape can be expressed as

$$R(\phi) = \begin{cases} R_0 \sum a_i \cos^i \phi, & \cos \phi \geq 0 \\ R_0 \sum b_i \cos^i \phi, & \cos \phi < 0 \end{cases} \quad (2)$$

By setting  $a_0 = b_0 = 1$ , and  $a_1 = b_1 = 0$ , the norm direction is continuous and the cavity boundary is smooth. In addition, we should keep the boundary slow varying, so simply we cut off the high order terms, only keep  $a_2(b_2)$  and  $a_3(b_3)$  nonzero [34]. Also, to break Y-axis symmetry, it needs  $a_2 \neq b_2$  or/and  $a_3 \neq -b_3$ . Moreover, we can set  $b_2 = b_3 = 0$  and  $a_2 + a_3 < 0$  to form Gibbous shape for further simplification.

For the this kind of Gibbous shape cavity with high refractive index material, there will always exist stable and unstable period-3 orbits with vertexes near  $(0, 2\pi/3, 4\pi/3)$  and  $(\pi/3, \pi, 5\pi/3)$ , respectively. By randomly set the parameters  $a_i$ , we can always get similar phase space structures to Fig. 1(c) in any Gibbous-shaped cavity. That is because, without Y-axis symmetric, the two sets of period-3 orbits in Gibbous shape cavities always have smaller convex angles near  $\pi/2$  in real space. Correspondingly, the fixed points of manifolds and stable islands are lower in phase space, which make the refraction regions fixed at about  $\phi \approx \pi/2$  and  $3\pi/2$  and unidirectional emission from the first refraction region. We carried out ray and wave simulations on lots of Gibbous shape cavities. Results indicate the single emission with far field divergence angle ranges from 20 to 50 degrees, confirming to

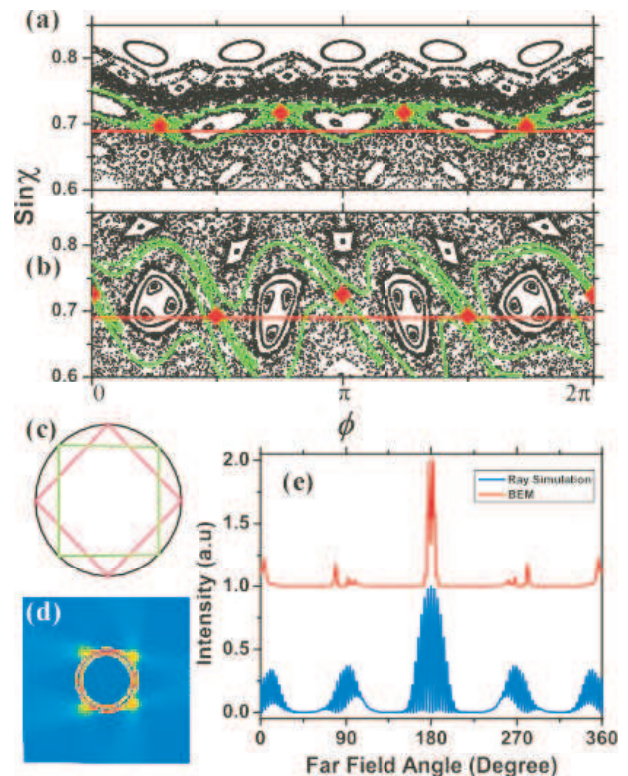


FIG. 2: (color online)(a) (b) the SOS of two cavities (a) HQHC  $\epsilon = 0.05$  and (b) the cavity shape support stable rectangle orbit and unidirectional emission designed in the text. (c) the rectangle and diamond shape period-4 orbits in the X-symmetric cavity. (d) The near field distribution of the unidirectional emission with  $kr \approx 52.5284$ . (e) The far field pattern of the cavity, red line is the ray simulation result (lifted by 1), and the blue line is corresponding to the result in (d).

our conjecture from the orbits. We find the cavity with  $a_2 = 0.0486$ ,  $a_3 = -0.1258$  gives good unidirectional far field pattern. The wave simulation gives a high Q ( $Q = 5.78 \times 10^6$ ) TM polarized WG mode with  $kr \approx 25.1842$ , and the far field divergence is only about 24 degrees, which is much smaller, comparing to 40 degrees reported in limaçon cavity [20].

Thus, we have shown how to get unidirectional emission in the Gibbous-shaped cavity. The limaçon cavity [20], as well as the cavity in Song's experiments [21], is a generalized Gibbous-shaped cavity. Their mechanisms for unidirectional emission can also be explained with our approach.

Now, we will generalize the above mechanism for unidirectional emission to low refractive index microcavities. Here we take the silica ( $n = 1.45$ ) for example. Similar to the period-3 orbits in high index cavities, the silica cavity's directional emission is basically influenced by period-4 orbits. The former experimental study on HQHC micro-sphere showed that the emission direction could be reduced to 2 nearly perpendicular direction [24]. The SOS of such HQHC is present in Fig. 2(a), where the stable period-4 islands [the red diamond orbit in Fig.2(c)] around the critical line prevent the rays unidirectional emission around  $\phi = \pi/2$ .

A strategy to solve the problem in this low index cavity is

to find a shape with stable islands away from  $\pi/2$ . That is to make the green rectangle period-4 orbit be stable and the red diamond orbit be unstable. Corresponding SOS is presented in Fig. 2(b). Rays can go cross the critical line near  $\pi/2$ . Similar to the analysis in high index cavity, the conditions for unidirectional emission in silica microcavity is: (i) The cavity supports the stable rectangle orbit. (ii) The stable island near  $\phi = 3\pi/4$  and  $5\pi/4$  is lower, and the fixed point (the red triangle in SOS) is lower near  $\phi = \pi/2$ .

In the numerical simulation of ray dynamics, we randomly choose parameters to set the boundary shape, judge that the rectangle orbit stable or not, and compare the islands position in SOS to fulfill the condition (ii). We can easily find a good cavity shape with  $a_2 = -0.1329, a_3 = 0.0948, b_2 = -0.0642, b_3 = -0.0224$  satisfies the above conditions, and gives good unidirectional far field pattern. Fig. 2(b) and Fig. 2(d) shows the SOS and field distribution of TM mode. Fig.2(e) is the corresponding far field pattern compares to the ray simulation. As we expect, the Q factor is up to  $2.75 \times 10^6$  and divergence is only about 30 degree.

Thanks to the ray-wave correspondence, an efficient route to design a unidirectional emission cavity shape could be: using the ray dynamics to give the SOS of the selective boundary shape, predicting the emission properties, and carrying out the wave simulation to confirm it. Here, we only gives examples on the typically materials, such as semiconductor and silicon ( $n \approx 3.3$ ) and silica glass ( $n \approx 1.45$ ). Other popular solid materials for photonics have similar refractive index. There are also many materials not at this range, such as some doped glass with the refractive index around 2.0. We have also successfully designed the cavity shapes to achieve high Q and unidirectional emission (not presented here). By adjusting the periodic-3 orbits or periodic-4 orbits, we can get appropriate emission direction and expect the unidirectional emission in the materials with refractive index range from 1.4 to 4.

There are also some deviations between the simulations with ray and wave, especially when  $kr$  is small. The actions

of light could not totally be described by rays. Better ray-wave correspondence could be expected in larger cavity [23]. In smaller cavity, wave properties should be included, such as, the diffractions and interference. In microcavities, researches have illustrated that some modifications should be included in the ray dynamics [35], such as the corrected Fresnel's law at curve interface [36], the Goos-Hänchen shift [38] and the Fresnel Filtering effect [37].

In conclusion, we examined and presented the mechanism for high Q unidirectional emission WG modes in microcavities. Based on the necessary condition for the continuous and single axis symmetric boundary shape, we can well control the directional emission from ARC by setting appropriate boundary shape to adjust the stable islands and fixed points of unstable orbits in phase space. With the assistance of ray dynamics, it is easy to design fabrication-friendly simple cavity boundary shape to achieve high Q and unidirectional emission in different materials with the refractive index range from 1.4 to 4. We expect our approaches presented here to discuss the light in cavities can be applied to the study of the chaotic transport in two dimensional phase space [39], as well as other opening non-integrable systems, such as quantum dots and nano-structures.

#### Acknowledgments

C.-L. Zou thanks Juhee Yang and J. Wiersig for discussions. Financial support by the National fundamental Research Program of China under Grant No 2006CB921900; National Science Foundation of China under Grant No. 60537020 and 60621064; The Knowledge Innovation Project of Chinese Academy of Sciences & Chinese Academy of Sciences and International Partnership Project; Y. Yang is also funded by the China Postdoctoral Science Foundation. F.-W. Sun is also supported by the starting funds from USTC for new faculty.

- 
- [1] For a review, see *Optical Microcavities*, edited by K. J. Vahala (World Scientific, Singapore, 2004).
  - [2] A. Mekis, J. U. Nockel, G. Chen, A. D. Stone, and R. K. Chang, *Phys. Rev. Lett.* **75**, 2682(1885).
  - [3] C. Gmachl, *et. al.*, *Science* **280**, 1556(1998).
  - [4] S.-B. Lee, J.-H. Lee, J.-S. Chang, H.-J. Moon, S. W. Kim, and K. An, *Phys. Rev. Lett.* **88**, 033903 (2002).
  - [5] S. Lacey, H. Wang, D. H. Foster, and J. U. Nockel, *Phys. Rev. Lett.* **91**, 033902 (2003).
  - [6] Y.-F. Xiao, C.-H. Dong, Z.-F. Han, G.-C. Guo, and Y.-S. Park, *Opt. Lett.* **32**, 644-646 (2007).
  - [7] T. Fukushima, T. Tanaka, and T. Harayama, *Appl. Phys. Lett.* **86**, 171103(2005).
  - [8] W. Fang, A. Yamilov, and H. Cao, *Phys. Rev. A* **72**, 023815 (2005).
  - [9] M. Lebental, J. S. Lauret, R. Hierle, and J. Zyss, *Appl. Phys. Lett.* **88**, 031108(2006).
  - [10] Y. S. Park, A. K. Cook, and H. Wang, *Nano Lett.* **6**, 2075 (2006).
  - [11] J. Yang, *et. al.*, *Appl. Phys. Lett.* **93**, 0611010(2008).
  - [12] H.-J. Stöckmann, *Quantum Chaos* (Cambridge University Press, Cambridge 2000).
  - [13] S.-Y. Lee, S. Rim, J.-W. Ryu, T.-Y. Kwon, M. Choi, and C.-M. Kim, *Phys. Rev. Lett.* **93**, 164102 (2004)
  - [14] J. Wiersig, and J. Main, *Phys. Rev. E* **77**, 036205 (2008).
  - [15] G. D. Chern, H. E. Tureci, A. D. Stone, R. K. Chang, M. Kneissl, and N. M. Johnson, *Appl. Phys. Lett.* **83**, 1710 (2003).
  - [16] M. Hentschel, T.-Y. Kwon, M. A. Belkin, R. Audet, and F. Capasso, *Opt. Express* **17**, 10335(2009).
  - [17] M. S. Kurdonglyan, S.-Y. Lee, S. Rim, and C. -M. Kim, *Opt. Lett.* **29**, 2758(2004).
  - [18] J. Wiersig and M. Hentschel, *Phys. Rev. A* **73**, 031802(R) (2006).
  - [19] J.-W. Ryu, S.-Y. Lee, and S. W. kim, *Phys. Rev. A* **79**, 053858 (2009).
  - [20] J. Wiersig and M. Hentschel, *Phys. Rev. Lett.* **100**, 033901(2008).
  - [21] Q. Song, H. Cao, B. Liu, S. T. Ho, W. Fang, and G. S. Solomon,

- arXiv 0810.3923(2008).
- [22] C. Yan, *et al.*, Appl. Phys. Lett **94**,251101(2009).
- [23] S. Shinohara, M. Hentschel, J. Wiersig, T. Sasaki, and T. Harayama, arXiv 0908.2708(2009).
- [24] Y.-F. Xiao, C.-H. Dong, C.-L. Zou, Z.-F. Han, L. Yang, and G.-C. Guo, Opt. Lett. **34**, 509(2009).
- [25] J. U. Nöckel and A. Douglas Stone, Nature **385**, 45(1997).
- [26] H. G. L. Schwefel *et al.*, J. Opt. Soc. Am. B **21**, 923(2004);
- [27] V. A. Podolskiy and E. E. Narimanov, Opt. Lett. **30**, 474 (2005).
- [28] S. Shinohara, T. Fukushima, and T. Harayama, Phys. Rev. A **77**, 033807(2008).
- [29] S.-B. Lee, *et al.*, Phys. Rev. A **75**,011802(R) (2007).
- [30] C.-H. Dong *et al.* unpublished.
- [31] L. E. Reichl, *The Transition to Chaos in Conservative Classical Systems: Quantum Manifestations* (springer, New York, 1992).
- [32] J. Wiersig, J. Opt. A: Pure Appl. Opt. **5**, 53(2003).
- [33] C.-L. Zou *et al.*, Submitted.
- [34] It is not required for general cases. Here we just set the values of high orders zero for simplicity in simulation, as well as simplification in fabrication.
- [35] M. Hentschel, Adv. Sol. St. Phys. **48**, 293-304 (2009).
- [36] M. Hentschel and H. Schomerus, Phys. Rev. E **65**, 045603(R) (2002).
- [37] N. B. Rex, H. E. Tureci, H. G. L. Schwefel, R. K. Chang, and A. Douglas Stone, Phys. Rev. Lett. **88**, 094102 (2002).
- [38] H. Schomerus and M. Hentschel, Phys. Rev. Lett. **96**, 243903 (2006).
- [39] J.-B. Shim, *et al.*, Phys. Rev. Lett. **100**, 174102 (2008).